
TransGAN: Two Transformers Can Make One Strong GAN

Yifan Jiang¹ Shiyu Chang² Zhangyang Wang¹

Abstract

The recent explosive interest on transformers has suggested their potential to become powerful “universal” models for computer vision tasks, such as classification, detection, and segmentation. However, how further transformers can go - are they ready to take some more notoriously difficult vision tasks, e.g., generative adversarial networks (GANs)? Driven by that curiosity, we conduct the first pilot study in building a GAN **completely free of convolutions**, using only pure transformer-based architectures. Our vanilla GAN architecture, dubbed **TransGAN**, consists of a memory-friendly transformer-based generator that progressively increases feature resolution while decreasing embedding dimension, and a patch-level discriminator that is also transformer-based. We then demonstrate TransGAN to notably benefit from data augmentations (more than standard GANs), a multi-task co-training strategy for the generator, and a locally initialized self-attention that emphasizes the neighborhood smoothness of natural images. Equipped with those findings, TransGAN can effectively scale up with bigger models and high-resolution image datasets. Specifically, our best architecture achieves highly competitive performance compared to current state-of-the-art GANs based on convolutional backbones. Specifically, TransGAN sets **new state-of-the-art** IS score of 10.10 and FID score of 25.32 on STL-10. It also reaches competitive 8.64 IS score and 11.89 FID score on Cifar-10, and 12.23 FID score on CelebA 64×64 , respectively. We also conclude with a discussion of the current limitations and future potential of TransGAN. The code is available at <https://github.com/VITA-Group/TransGAN>.

¹Department of Electronic and Computer Engineering, University of Texas at Austin, Texas, USA ²IBM Research, Massachusetts, USA. Correspondence to: Yifan Jiang <yifan-jiang97@utexas.edu>.

1. Introduction

Generative adversarial networks (GANs) have gained considerable success on numerous tasks including image synthesis (Radford et al., 2015; Arjovsky et al., 2017; Gulrajani et al., 2017; Miyato et al., 2018; Brock et al., 2018), image translation (Isola et al., 2017; Zhu et al., 2017a;b; Chen et al., 2020b), and image editing (Yang et al., 2019; Jiang et al., 2021). Unfortunately, GANs suffer from the notorious training instability, and numerous efforts have been devoted to stabilizing GAN training, introducing various regularization terms (Kurach et al., 2019; Roth et al., 2017; Zhang et al., 2019b; Mescheder et al., 2018), better losses (Gulrajani et al., 2017; Mao et al., 2017; Jolicoeur-Martineau, 2018; Li et al., 2017), and training recipes (Salimans et al., 2016; Karras et al., 2017).

Another parallel route to improving GANs examines their *neural architectures*. (Lucic et al., 2018; Kurach et al., 2019) reported a large-scale study of GANs and observed that when serving as (generator) backbones, popular neural architectures perform comparably well across the considered datasets. Their ablation study suggested that most of the variations applied in the ResNet family architectures lead to marginal improvements in the sample quality. However, further research introduced neural architecture search (NAS) to GANs and suggests that enhanced backbone designs are also important for improving GANs further, just like for other computer vision tasks. Those works are consistently able to discover stronger GAN architectures beyond the standard ResNet topology (Gong et al., 2019; Gao et al., 2020; Tian et al., 2020). Other efforts include customized modules such as self-attention (Zhang et al., 2019a), style-based generator (Karras et al., 2019), and autoregressive transformer-based part composition (Esser et al., 2020).

However, there is one last “commonsense” that seems to have seldomly been challenged: using convolutional neural networks (CNNs) as GAN backbones. The original GAN (Goodfellow et al., 2014; Denton et al., 2015) used fully-connected networks and can only generate small images. DCGAN (Radford et al., 2015) was the first to scale up GANs using CNN architectures, which allowed for stable training for higher resolution and deeper generative models. Since then, in the computer vision domain, nearly every successful GAN relies on CNN-based generators and dis-

criminators. Convolutions, with the strong inductive bias for natural images, crucially contribute to the appealing visual results and rich diversity achieved by modern GANs.

Can we build a strong GAN completely free of convolutions? This is a question not only arising from intellectual curiosity, but also of practical relevance. Fundamentally, a convolution operator has a local receptive field, and hence CNNs cannot process long-range dependencies unless passing through a sufficient number of layers. However, that could cause the loss of feature resolution and fine details, in addition to the difficulty of optimization. Vanilla CNN-based models (including conventional GANs) are therefore inherently not well suited for capturing an input image’s “global” statistics, as demonstrated by the benefits from adopting self-attention (Zhang et al., 2019a) and non-local (Wang et al., 2018b) operations in computer vision.

We are inspired by the emerging trend of using Transformer architectures for computer vision tasks (Carion et al., 2020; Zeng et al., 2020; Dosovitskiy et al., 2020). Transformers (Vaswani et al., 2017; Devlin et al., 2018) have prevailed in natural language processing (NLP), and lately, start to perform comparably or even better than their CNN competitors in a variety of vision benchmarks. The charm of the transformer to computer vision lies in at least two-fold: (1) it has strong representation capability and is free of human-defined inductive bias. In comparison, CNNs exhibit a strong bias towards feature locality, as well as spatial invariance due to sharing filter weights across all locations; (2) the transformer architecture is general, conceptually simple, and has the potential to become a powerful “universal” model across tasks and domains (Dosovitskiy et al., 2020). It can get rid of many ad-hoc building blocks commonly seen in CNN-based pipelines (Carion et al., 2020).

1.1. Our Contributions

This paper aims for the first pilot study to build a GAN completely free of convolutions, using only pure transformer-based architecture. Our ambitious goal is clearly distinguished from the previous works that only applied self-attention or transformer encoder block in conjunction with CNN-based generative models (Zhang et al., 2019a; Esser et al., 2020). However, as all previous pure transformer-based models in computer vision are focused on discriminative tasks such as classification and detection, our goal faces several daunting gaps ahead. First and foremost, although a pure transformer architecture applied directly to sequences of image patches can perform very well on image classification tasks (Dosovitskiy et al., 2020), it is unclear whether the same way remains effective in generating images, which poses a high demand for spatial coherency in structure, color, and texture. The handful of existing transformers that output images have unanimously leveraged CNN-based part

encoders (Esser et al., 2020) or convolutional feature extractors (Yang et al., 2020; Chen et al., 2020a). Moreover, even given well-designed CNN-based architectures, training GANs is notoriously unstable and prone to mode collapse (Salimans et al., 2016). Training visual transformers are also known to be tedious, heavy, and data-hungry (Dosovitskiy et al., 2020). Mingling the two will undoubtedly amplify the challenges of training.

In view of those challenges, this paper presents a coherent set of efforts and innovations towards building the **pure** transformer-based GAN architectures, dubbed **TransGAN**. A naive option may directly stack multiple transformer blocks from raw pixel inputs, but that would require prohibitive memory and computation. Instead, we start with a memory-friendly transformer-based generator by gradually increasing the feature map resolution while decreasing the embedding dimension in each stage. The discriminator, also transformer-based, tokenizes the image patches rather than pixels as its inputs and classifies between real and fake images. This vanilla TransGAN architecture naturally inherits the advantages of the global receptive field by the self-attention, but practically it leads to degraded generation and broken visual smoothness. To close the performance gap between CNN-based GANs, we then demonstrate TransGAN to notably benefit from data augmentations (more than standard GANs), a multi-task co-training strategy with a self-supervised auxiliary loss, and a locally initialized self-attention that emphasizes the neighborhood smoothness of natural images. Our contributions are outlined below:

- **Model Architecture:** We build the first GAN using purely transformers and no convolution. To avoid overwhelming memory overheads, we create a memory-friendly generator and a patch-level discriminator, both transformer-based without bells and whistles. TransGAN can be effectively scaled up to larger models.
- **Training Technique:** We study a number of techniques to train TransGAN better, ranging from data augmentation, multi-task co-training for generator with self-supervised auxiliary loss, and localized initialization for self-attention. Extensive ablation studies, discussions, and insights are presented. None of them requires any architecture change.
- **Performance:** TransGAN achieves highly competitive performance compared to current state-of-the-art CNN-based GANs. Specifically, it sets new state-of-the-art IS score of 10.10 and FID score of 25.32 on STL-10 and also reaches competitive 8.64 IS score and 11.89 FID score on Cifar-10, and 12.23 FID score on CelebA 64×64 , respectively. We also summarize the current limitations and future potential of TransGAN.

2. Relative Works

2.1. Generative Adversarial Networks

GANs (Gui et al., 2020) can be generalized to minimizing a large family of divergences, and are practically formulated as minimax optimization. After its origin, GANs quickly embrace fully convolutional backbones (Radford et al., 2015), and inherited most successful designs from CNNs such as batch normalization, pooling, ReLU/Leaky ReLU and more. GANs are widely adopted in image-to-image translation (Isola et al., 2017; Zhu et al., 2017a), image enhancement (Jiang et al., 2021; Ledig et al., 2017; Kupyn et al., 2018), and image editing (Ouyang et al., 2018; Yu et al., 2018). To alleviate its unstable training, a number of techniques have been studied, including the Wasserstein loss (Arjovsky et al., 2017), the style-based generator (Karras et al., 2019), progressive training (Karras et al., 2017), and Spectral Normalization (Miyato et al., 2018).

2.2. Visual Transformer

The original transformer was built for NLP (Vaswani et al., 2017), where the multi-head self-attention and feed-forward MLP layer are stacked to capture the long-term correlation between words. Its popularity among computer vision tasks rises recently (Parmar et al., 2018; Yang et al., 2020; Zeng et al., 2020; Carion et al., 2020; Wu et al., 2020; Chen et al., 2020a). The core of a transformer is the self-attention mechanism, which characterizes the dependencies between any two distant tokens. It could be viewed as a special case of non-local operations in the embedded Gaussian (Wang et al., 2018b), that captures long-range dependencies of pixels in image/video. A recent work (Dosovitskiy et al., 2020) implements highly competitive ImageNet classification using pure transformers, by treating an image as a sequence of 16×16 visual words. However, its success relies on pre-training on large-scale external data. (Touvron et al., 2020) improves the data efficiency for its training. Besides image classification task, transformer and its variants are also explored on image processing (Chen et al., 2020a), point cloud (Zhao et al., 2020a), object detection (Carion et al., 2020; Zhu et al., 2020) and so on. A comprehensive review is referred to (Han et al., 2020).

2.3. Transformer Modules for Image Generation

There exist several related works combining the transformer modules into image generation models, by replacing certain components of CNNs. (Parmar et al., 2018) firstly formulated image generation as autoregressive sequence generation, for which they adopted a transformer architecture. (Child et al., 2019) propose sparse factorization of the attention matrix to reduce its complexity. While those two works did not tackle the GANs, one recent (concurrent) work (Esser et al., 2020) used a convolutional GAN to

learn a codebook of context-rich visual parts, whose composition is subsequently modeled with an autoregressive transformer architecture. The authors demonstrated success in synthesizing high-resolution images. However, the overall CNN architecture remains in place (including CNN encoder/decoder for the generators, and a fully CNN-based discriminator), and the customized designs (e.g. codebook and quantization) also limit their model’s versatility. To our best knowledge, no existing work has tried to completely remove convolutions from their generative frameworks.

3. Technical Approach: A Journey Towards GAN with Pure Transformers

A GAN consists of a generator G and a discriminator D . We start by replacing G or D with a transformer to understand the design sensitivity; then we replace both of them and optimize our design for memory efficiency. On top of the vanilla TransGAN with both G and D being transformers, we gradually introduce a series of training techniques to fix its weakness, including data augmentation, an auxiliary task for co-training, and injecting locality to self-attention. With those aids, TransGAN can be scaled up to deeper/wider models, and generate images of high quality.

3.1. Vanilla Architecture Design for TransGAN

3.1.1. TRANSFORMER ENCODER AS BASIC BLOCK

We choose the transformer encoder (Vaswani et al., 2017) as our basic block, and try to make minimum changes. An encoder is a composition of two parts. The first part is constructed by a multi-head self-attention module and the second part is a feed-forward MLP with GELU non-linearity. We apply layer normalization (Ba et al., 2016) before both of the two parts. Both parts employ residual connection.

3.1.2. MEMORY-FRIENDLY GENERATOR

Transformers in NLP taking each word as inputs (Devlin et al., 2018). However, if we similarly generate an image in a pixel-by-pixel manner through stacking transformer encoders, even a low-resolution image (e.g. 32×32) can result in a long sequence (1024), and then even more explosive cost of self-attention (quadratic w.r.t. the sequence length). To avoid this prohibitive cost, we are inspired by a common design philosophy in CNN-based GANs, to iteratively up-scale the resolution at multiple stages (Denton et al., 2015; Karras et al., 2017). Our strategy is to gradually increase the input sequence and reduce the embedding dimension.

As shown in Fig.1 left, we propose a memory-friendly transformer-based generator that consists of multiple stages (default 3 for CIFAR-10). Each stage stacks several encoder blocks (5, 2, and 2 by default). By stages, we gradually

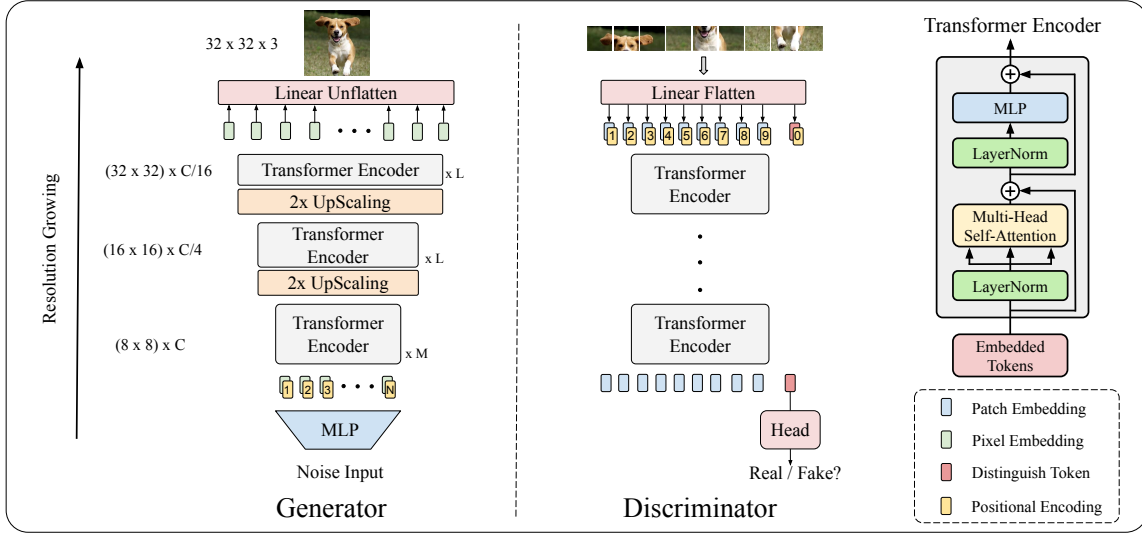


Figure 1. The pipeline of the pure transform-based generator and discriminator of TransGAN. Here $H = W = 8$ and $H_T = W_T = 32$. We show 9 patches for discriminator as an example while in practice we always use 8×8 patches across all datasets.

increase the feature map resolution until it meets the target resolution $H_T \times W_T$. Specifically, the generator takes the random noise as its input, and passes it through a multiple-layer perceptron (MLP) to a vector of length $H \times W \times C$. The vector is reshaped into a $H \times W$ resolution feature map (by default we use $H = W = 8$), each point a C -dimensional embedding. This “feature map” is next treated as a length-64 sequence of C -dimensional tokens, combined with the learnable positional encoding.

Similar to BERT (Devlin et al., 2018), the transformer encoders take embedding tokens as inputs and calculate the correspondence between each token recursively. To synthesize higher resolution images, we insert an upsampling module after each stage, consisting of a reshaping and `pixelshuffle` (Shi et al., 2016) module. The upsampling module firstly reshapes the 1D sequence of token embedding back to a 2D feature map $X_0 \in R^{H \times W \times C}$ and then adopt the `pixelshuffle` module to upsample its resolution and downsample the embedding dimension, resulting in the output $X'_0 \in R^{2H \times 2W \times C/4}$. After that, the 2D feature map X'_0 is again reshaped into the 1D sequence of embedding tokens where the token number becomes $4HW$ and the embedding dimension is $C/4$. Therefore, at each stage the resolution (H, W) becomes 2 times larger, while the embedded dimension C is reduced to a quarter of the input. This trade-off mitigates the memory and computation explosion. We repeat multiple stages until the resolution reaches (H_T, W_T) , and then we will project the embedding dimension to 3 and obtain the RGB image $Y \in R^{H_T \times W_T \times 3}$.

3.1.3. TOKENIZED-INPUT FOR DISCRIMINATOR

Unlike the generator which needs to synthesize each pixel precisely, the discriminator is only expected to distinguish between real/fake images. This allows us to semantically tokenizing the input image into the coarser patch-level (Dosovitskiy et al., 2020). As shown in Fig. 1 right, the discriminator takes the patches of an image as inputs. Following (Dosovitskiy et al., 2020), we split the input images $Y \in R^{H \times W \times 3}$ into 8×8 patches where each patch can be regarded as a “word”. The 8×8 patches are then converted to the 1D sequence of token embeddings through a linear flatten layer, with token number $N = 8 \times 8 = 64$ and embedding dimension equal to C . After that, the learnable positional encoding is added and a `[cls]` token is appended at the beginning of the 1D sequence. After passing through the transformer encoders, only `[cls]` token is taken by the classification head to output the real/fake prediction.

3.1.4. EVALUATION OF TRANSFORMER-BASED GAN

To put the performance of transformer-based generator G and discriminator D into context, we take a reference to one of the state-of-the-art GANs, AutoGAN (Gong et al., 2019), which has convolutional G and D . We study four combinations: i) AutoGAN G + AutoGAN D (i.e., original AutoGAN); ii) Transformer G + AutoGAN D ; iii) AutoGAN G + Transformer D ; and iv) Transformer G + Transformer D (i.e., our vanilla TransGAN). Our transformer G has $\{5, 2, 2\}$ encoder blocks in each stage and transformer D only has one stage with 7 encoder blocks. For all models, we train them on CIFAR-10 to evaluate Inception Score (Salimans et al., 2016) and FID (Heusel et al., 2017). We try our best

on tuning hyperparameters to reach their best performance, detailed setting is shown in the Appendix. A.1. Table 1 reveals a few very intriguing findings:

- Transformer-based G has a strong capacity: when training with the mature AutoGAN D , its performances already get on par with the original AutoGAN. That is also aligned with (Esser et al., 2020) who found putting transformers in the generator is successful.
- However, Transformer-based D seems to be an inferior “competitor” and unable to push AutoGAN G towards good generation results. After replacing AutoGAN G with Transformer G , the results slightly improves, possibly benefiting more symmetric G and D structures. However, the numbers still largely lag behind when using convolutional D .

Note that although not yet a pure transformer, the promising result of Transformer G + AutoGAN D already has practical relevance - considering in most GAN applications, the discriminator is discarded after training and only the generator is kept for testing use. If one’s goal is to simply obtain a transformer-based G , then the goal can be fulfilled by Transformer G + AutoGAN D . However, for our much more ambitious goal of making GAN completely free of convolutions, our journey has to continue.

Table 1. Inception Score (IS) and FID results on CIFAR-10. The first row shows the AutoGAN results (Gong et al., 2019); the second and thirds row show the mixed transformer-CNN results; and the last row shows the pure-transformer GAN results.

GENERATOR	DISCRIMINATOR	IS \uparrow	FID \downarrow
AUTOGAN	AUTOGAN	8.55 \pm 0.12	12.42
TRANSFORMER	AUTOGAN	8.59\pm 0.10	13.23
AUTOGAN	TRANSFORMER	6.17 \pm 0.12	49.83
TRANSFORMER	TRANSFORMER	6.95 \pm 0.13	41.41

3.2. Data Augmentation is Crucial for TransGAN

The preliminary findings in Table 1 inspire us to reflect on the key barrier - it seems that D is not well trained, no matter with CNN- or transformer-based G . Note the transformer-based classifiers were known to be highly data-hungry (Dosovitskiy et al., 2020) due to the removal of human-designed bias: they were inferior to CNNs until much larger external data was used for pre-training. To remove this roadblock, data augmentation was revealed as a blessing in (Touvron et al., 2020), which showed that different types of strong data augmentation can lead us to data-efficient training for visual transformers.

Traditionally, contrary to training image classifiers, training GANs hardly refers to data augmentation. Lately, there is

an interest surge in training GANs in the “few-shot” regime, aiming to match state-of-the-art GAN results with orders of magnitude fewer real images, using well-crafted data augmentation (Zhao et al., 2020b; Karras et al., 2020a).

We target in a different setting: comparing the influence of data augmentation for CNN- and transformer-based GANs, in the full-data regime. We use the whole training set of CIFAR-10, and compare TransGAN with three state-of-the-art CNN-based GANs: WGAN-GP (Gulrajani et al., 2017), AutoGAN and StyleGAN v2 (Karras et al., 2020b). The data augmentation method is DiffAug (Zhao et al., 2020b).

Table 2. The effectiveness of Data Augmentation (DA) on both CNN-based GANs and TransGAN. We used the full CIFAR-10 training set and DiffAug (Zhao et al., 2020b).

METHODS	DA	IS \uparrow	FID \downarrow
WGAN-GP (GULRAJANI ET AL., 2017)	\times \checkmark	6.49 \pm 0.09 6.29 \pm 0.10	39.68 37.14
AUTOGAN (GONG ET AL., 2019)	\times \checkmark	8.55 \pm 0.12 8.60 \pm 0.10	12.42 12.72
STYLEGAN v2 (ZHAO ET AL., 2020B)	\times \checkmark	9.18 9.40	11.07 9.89
TRANSGAN	\times \checkmark	6.95 \pm 0.13 8.15 \pm 0.14	41.41 19.85

As shown in Table. 2, for three CNN-based GANs, the performance gains of data augmentation seems to diminish in the full-data regime. Only the largest model StyleGAN-V2 seems to gain visibly in both IS and FID. In sharp contrast, TransGAN, also trained on the same training set, sees a shockingly large margin of improvement: IS improving from 6.95 to 8.15 and from 41.41 to 19.85, respectively. That re-confirms the findings (Dosovitskiy et al., 2020; Touvron et al., 2020) that transformer-based architectures are much more data-hungry than CNNs, and that can be helped by stronger data augmentation to a good extent.

3.3. Co-Training with Self-Supervised Auxiliary Task

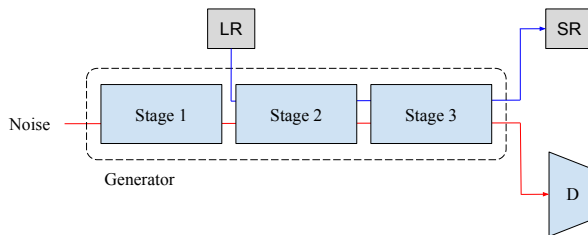


Figure 2. Co-training the transformer G with an auxiliary task of super resolution. “LR” and “SR” represent low-resolution input and high-resolution output respectively.

Transformers in the NLP domain benefit from multiple pre-training tasks (Devlin et al., 2018; Song et al., 2020). In-

terestingly, adding a self-supervised auxiliary task (e.g., rotation prediction) was previously found to stabilize GAN training too (Chen et al., 2019). That makes it a natural idea to incorporate self-supervised auxiliary co-training into TransGAN, which may help it capture more image priors.

Specifically, we construct an auxiliary task of *super resolution*, in addition to the GAN loss. This task comes “for free”, since we can just treat the available real images as high-resolution, and downsample them to obtain low-resolution counterparts. The generator loss is added with a auxiliary term $\lambda * L_{SR}$, where L_{SR} is the mean-square-error (MSE) loss and the coefficient λ is empirically set as 50. Figure 2 illustrates the idea of multi-task co-training (MT-CT), and it improves TransGAN from 8.15 IS and 19.85 FID to 8.20 IS and 19.12 FID, respectively, as in Table 3.

Table 3. Ablation studies for multi-task co-training (MT-CT) and locality-aware self-attention initialization on TransGAN.

MODEL	IS \uparrow	FID \downarrow
TRANSGAN + DA (*)	8.15 \pm 0.14	19.85
(*) + MT-CT	8.20 \pm 0.14	19.12
(*) + MT-CT + LOCAL INIT.	8.22\pm 0.12	18.58

3.4. Locality-Aware Initialization for Self-Attention

CNN architectures have the built-in prior of natural image smoothness (Ulyanov et al., 2018) which was believed to contribute to natural image generation. That was lacked by the transformer architecture which features full learning flexibility. However, (Dosovitskiy et al., 2020) observed that transformers still tend to learn convolutional structures from images. Therefore, a meaningful question arises as, whether we can efficiently encode inductive image biases while still retaining the flexibility of transformers. (Esser et al., 2020) pursued so by keeping a convolutional architecture to encode the low-level image structure. In this paper, we show that a similar effect may be achieved without changing the pure transformer architecture at all, yet instead by warm-starting the self-attention properly.

To inject this particular prior, we introduce the locality-aware initialization for self-attention. Our specific strategy is illustrated in Figure 3. We introduce a mask by which each query is only allowed to interact with its local neighbors that are not “masked”. Different from previous methods (Daras et al., 2020; Parmar et al., 2018; Child et al., 2019; Beltagy et al., 2020) during training we gradually reduce the mask until diminishing it, and eventually the self-attention is fully global¹. That strategy stems from our observation that a

¹Implementation-wise, we control the window size for the allowable interactive neighborhood tokens. The window size is 8 for epochs 0-20, then 10 for epochs 20-30, 12 for epochs 30-40, 14 for epochs 40-50, and then the full image all afterward.

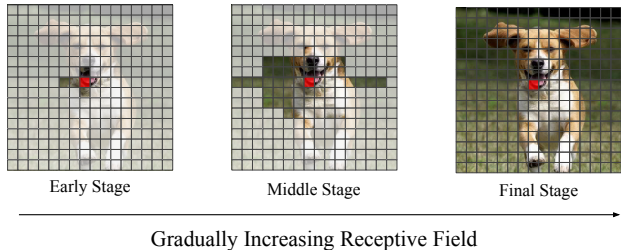


Figure 3. Locality-aware initialization for self-attention. The red block indicates a query location, the transparent blocks are its allowable key locations to interact with, and the gray blocks indicate the masked region. TransGAN gradually increases the allowable region during the training process.

localized self-attention (Parmar et al., 2018) is most helpful at the early training stage, but can hurt the later training stage and the final achievable performance. We consider this locality-aware initialization as a regularizer that comes for the early training dynamics and then gradually fades away (Golatkar et al., 2019). It will enforce TransGAN to learn image generation, by prioritizing on the local neighborhood first (which provides the “necessary details”), followed by exploiting non-local interactions more broadly (which may supply more “finer detail” and also noise). Table 3 shows that it improves both IS and (more notably) FID.

3.5. Scaling up to Large Models

All previous training techniques have contributed to a better and more stable TransGAN, consisting of only transformer-based G and D . Equipped with them all (DA, MT-CT, and Local Init.), we are now ready to scale TransGAN up and see how much further we could gain from bigger models.

As shown in Table 4, we firstly enlarge the embedded dimension of the transformer-based G , from (default) 384 to 512 and then 768², and denote the resultant models as *TransGAN-S*, *TransGAN-M* and *TransGAN-L*, respectively. That comes with a consistent and remarkable gain in IS (up to 0.28), and especially FID (up to 4.08) – without any extra hyperparameter tuning.

We then increase the depth (number of transformer encoder blocks) on top of *TransGAN-L*. The original transformer G has {5,2,2} encoder blocks in each stage. We increase the number of encoder blocks to {5,4,2} and the embedded dimension to 1024 as well, obtaining *TransGAN-XL* from *TransGAN-L*. Still, both IS and FID benefit, and FID is reduced by another 2.57.

²We find enlarging G to significantly improve performance, while enlarging D seems to have negligible impact. Therefore, we increase G size by default and keep D the same.

Table 4. Scaling-up the model size of TransGAN on Cifar-10. Here “Dim” represents the embedded dimension of transformer and “Depth” is the number of transformer encoder block in each stage.

MODEL	DEPTH	DIM	IS \uparrow	FID \downarrow
TRANSKAN-S	{5,2,2}	384	8.22 \pm 0.14	18.58
TRANSKAN-M	{5,2,2}	512	8.36 \pm 0.12	16.27
TRANSKAN-L	{5,2,2}	768	8.50 \pm 0.14	14.46
TRANSKAN-XL	{5,4,2}	1024	8.63 \pm 0.16	11.89

4. Comparison with State-of-the-art GANs

Datasets We adopt CIFAR-10 (Krizhevsky et al., 2009) dataset as the main evaluation benchmark during the ablation study. The CIFAR-10 dataset consists of 60k 32x32 color images in 10 classes, with 50k training images and 10k testing images respectively. We follow the standard setting that the 50k training images without labels are used for training the TransGAN, where each image is resized to 32×32 resolution.

We further consider the STL-10 (Coates et al., 2011) and CelebA (Liu et al., 2015) dataset to scale up the TransGAN to higher resolution image synthesis tasks. For the STL-10 dataset, we use both the 5k training images and 100k unlabeled images for training our TransGAN. Each image is resized to 48×48 resolution. For the CelebA dataset, we use 200k unlabeled face images with their aligned and cropped version. We provide the 64×64 resolution results in the experiments.

Implementation We follow the training setting of WGAN (Arjovsky et al., 2017). The learning rate of both generator and discriminator are set to $1e-4$, using the Adam optimizer, where a batch size of 64 is set for discriminator and 128 for generator. For higher resolution (64×64) experiments, their batch sizes decrease to 16 and 32 respectively to fit the GPU memory. Similar to (Karras et al., 2017), we include an extra term with an extremely small weight for the discriminator loss to avoid loss explosion. We use 4 V100 GPUs for all experiments by default. The training process takes 2 days on Cifar-10 and 3 days on STL-10 and CelebA. Our main results are under the unconditional image synthesis setting.

4.1. Results on Cifar-10

We compare TransGAN with recently published results by ConvNet-based GANs on the CIFAR-10 dataset, shown in Table. 5. The results are all collected from the original papers with their best hand-tuned training settings.

As shown in Table. 5, TransGAN surpasses the strong AutoGAN (Gong et al., 2019) and many other latest competitors such as SN-GAN (Miyato et al., 2018), improving MMD-GAN (Wang et al., 2018a), and MGAN (Hoang et al., 2018),

Table 5. Unconditional image generation results on Cifar-10.

METHODS	IS	FID
WGAN-GP (GULRAJANI ET AL., 2017)	6.49 \pm 0.09	39.68
LRGAN (YANG ET AL., 2017)	7.17 \pm 0.17	-
DFM (WARDE-FARLEY & BENGIO, 2016)	7.72 \pm 0.13	-
SPLITTING GAN (GRINBLAT ET AL., 2017)	7.90 \pm 0.09	-
IMPROVING MMD-GAN (WANG ET AL., 2018A)	8.29	16.21
MGAN (HOANG ET AL., 2018)	8.33 \pm 0.10	26.7
SN-GAN (MIYATO ET AL., 2018)	8.22 \pm 0.05	21.7
PROGRESSIVE-GAN (KARRAS ET AL., 2017)	8.80 \pm 0.05	15.52
AUTOGAN (GONG ET AL., 2019)	8.55 \pm 0.10	12.42
STYLEGAN V2 (ZHAO ET AL., 2020B)	9.18	11.07
TRANSKAN-XL	8.63 \pm 0.16	11.89

in terms of inception score (IS); it is only next to the huge and highly-engineered Progressive GAN and StyleGAN v2.

Comparing the FID results, TransGAN is even found to outperform Progressive GAN, while being slightly inferior to StyleGANv2 (Karras et al., 2020b). The visual examples generated on CIFAR-10 are shown in Fig. 4.

4.2. Results on STL-10

We then apply the proposed TransGAN on another popular benchmark STL-10, with 48×48 resolution. We increase the input feature map of the generator’s first stage from $(8 \times 8) = 64$ to $(12 \times 12) = 144$ to fit the target resolution. Then the proposed TransGAN-XL is compared with both the automatic searched ConvNets and hand-crafted ConvNets, shown in Table. 6.

Different from the results on Cifar-10, we find that TransGAN outperforms all current models and sets new state-of-the-art results in terms of both IS and FID score. This is due to that the dataset size of STL-10 is $2 \times$ larger than Cifar-10, demonstrating our assumption that transformer-based architecture is much more data-hungry than ConvNets. The visual examples generated on STL-10 are shown in Fig. 4.

4.3. Generation on Higher Resolution

As TransGAN achieves highly promising results on the standard benchmarks of Cifar-10 and STL-10, we continue to push TransGAN to the more challenging dataset, CelebA 64×64 . To synthesize 64×64 output images, we increase



Figure 4. Visual Results of TransGAN on Cifar-10, STL-10, and CeleBA 64×64 .

Table 6. Unconditional image generation results on STL-10.

METHODS	IS	FID
DFM (WARDE-FARLEY & BENGIO, 2016)	8.51 ± 0.13	-
D2GAN (NGUYEN ET AL., 2017)	7.98	-
PROBGAN (HE ET AL., 2019)	8.87 ± 0.09	47.74
DIST-GAN (TRAN ET AL., 2018)	-	36.19
SN-GAN (MIYATO ET AL., 2018)	9.16 ± 0.12	40.1
IMPROVING MMD-GAN (WANG ET AL., 2018A)	9.23 ± 0.08	37.64
AUTOGAN (GONG ET AL., 2019)	9.16 ± 0.12	31.01
ADVERSARIALNAS-GAN (GAO ET AL., 2020)	9.63 ± 0.19	26.98
TRANSKAN-XL	10.10 ± 0.17	25.32

the stage number of the generator from 3 to 4 while the new generator contains $\{5, 3, 3, 2\}$ encoder blocks in each stage. Detailed network configurations are included in the Appendix. B. Without any further hyper-parameter tuning, TransGAN-XL reaches a FID of 12.23, demonstrating its applicability on higher resolution tasks. The visual results are shown in Fig. 4, and more baseline comparison results are included in the Appendix. ?? due to the space limit.

5. Conclusions, Limitations, and Discussions

We have proposed TransGAN, a new GAN paradigm based on pure transformers. We have carefully crafted the architectures and thoughtfully designed training techniques. As a result, TransGAN has achieved comparable performance to some state-of-the-art CNN-based GAN methods across multiple popular datasets. We show that the traditional re-

liance on CNN backbones and many specialized modules may not be necessary for GANs, and pure transformers can be sufficiently capable for image generation.

The pure transformer-based architecture brings versatility to TransGAN. As we turn from specialized to general-purpose architectures, one strong motivation is to simplify and unify various task pipelines, so one general suite of models could be extensively reused by many applications, avoiding the need of re-inventing wheels. There is an appealing potential that many associated techniques developed for improving transformers, originally proposed for NLP applications, could become available to TransGAN as well.

Building a GAN using only transformers appears to be more challenging than other transformer-based vision models (Dosovitskiy et al., 2020), due to the higher bar for realistic image generation (compared to classification) and the high instability of GAN training itself. Considering that existing transformer-based models (Carion et al., 2020; Dosovitskiy et al., 2020) are mostly on par or slightly inferior to their strongest CNN competitors (assuming no extra data used), we find TransGAN to provide an encouraging starting point.

Still, there is a large room for TransGAN to improve further, before it can outperform the best hand-designed GANs with more margins. We point out a few specific items that call for continuing efforts:

- More sophisticated tokenizing for both G and D , e.g. using some semantic grouping (Wu et al., 2020).
- Pre-training transformers using pretext tasks (Dai et al., 2020), which may improve over our current MT-CT.
- Stronger attention forms, e.g., (Zhu et al., 2020).
- More efficient self-attention forms (Wang et al., 2020; Choromanski et al., 2020), which not only help improve the model efficiency, but also save memory costs and hence help higher-resolution generation.

References

- Arjovsky, M., Chintala, S., and Bottou, L. Wasserstein gan. *arXiv preprint arXiv:1701.07875*, 2017.
- Ba, J. L., Kiros, J. R., and Hinton, G. E. Layer normalization. *arXiv preprint arXiv:1607.06450*, 2016.
- Beltagy, I., Peters, M. E., and Cohan, A. Longformer: The long-document transformer. *arXiv preprint arXiv:2004.05150*, 2020.
- Brock, A., Donahue, J., and Simonyan, K. Large scale gan training for high fidelity natural image synthesis. *arXiv preprint arXiv:1809.11096*, 2018.
- Carion, N., Massa, F., Synnaeve, G., Usunier, N., Kirillov, A., and Zagoruyko, S. End-to-end object detection with transformers. *arXiv preprint arXiv:2005.12872*, 2020.
- Chen, H., Wang, Y., Guo, T., Xu, C., Deng, Y., Liu, Z., Ma, S., Xu, C., Xu, C., and Gao, W. Pre-trained image processing transformer. *arXiv preprint arXiv:2012.00364*, 2020a.
- Chen, H., Wang, Y., Shu, H., Wen, C., Xu, C., Shi, B., Xu, C., and Xu, C. Distilling portable generative adversarial networks for image translation. In *Proceedings of the AAAI Conference on Artificial Intelligence*, volume 34, pp. 3585–3592, 2020b.
- Chen, T., Zhai, X., Ritter, M., Lucic, M., and Houlshby, N. Self-supervised gans via auxiliary rotation loss. In *Proceedings of the IEEE/CVF Conference on Computer Vision and Pattern Recognition*, pp. 12154–12163, 2019.
- Child, R., Gray, S., Radford, A., and Sutskever, I. Generating long sequences with sparse transformers. *arXiv preprint arXiv:1904.10509*, 2019.
- Choromanski, K., Likhoshesterov, V., Dohan, D., Song, X., Gane, A., Sarlos, T., Hawkins, P., Davis, J., Mohiuddin, A., Kaiser, L., et al. Rethinking attention with performers. *arXiv preprint arXiv:2009.14794*, 2020.
- Coates, A., Ng, A., and Lee, H. An analysis of single-layer networks in unsupervised feature learning. In *Proceedings of the fourteenth international conference on artificial intelligence and statistics*, pp. 215–223. JMLR Workshop and Conference Proceedings, 2011.
- Dai, Z., Cai, B., Lin, Y., and Chen, J. Up-detr: Unsupervised pre-training for object detection with transformers. *arXiv preprint arXiv:2011.09094*, 2020.
- Daras, G., Odena, A., Zhang, H., and Dimakis, A. G. Your local gan: Designing two dimensional local attention mechanisms for generative models. In *Proceedings of the IEEE/CVF Conference on Computer Vision and Pattern Recognition*, pp. 14531–14539, 2020.
- Denton, E., Chintala, S., Szlam, A., and Fergus, R. Deep generative image models using a laplacian pyramid of adversarial networks. *arXiv preprint arXiv:1506.05751*, 2015.
- Devlin, J., Chang, M.-W., Lee, K., and Toutanova, K. Bert: Pre-training of deep bidirectional transformers for language understanding. *arXiv preprint arXiv:1810.04805*, 2018.
- Dosovitskiy, A., Beyer, L., Kolesnikov, A., Weissenborn, D., Zhai, X., Unterthiner, T., Dehghani, M., Minderer, M., Heigold, G., Gelly, S., et al. An image is worth 16x16 words: Transformers for image recognition at scale. *arXiv preprint arXiv:2010.11929*, 2020.
- Esser, P., Rombach, R., and Ommer, B. Taming transformers for high-resolution image synthesis. *arXiv preprint arXiv:2012.09841*, 2020.
- Gao, C., Chen, Y., Liu, S., Tan, Z., and Yan, S. Adversarialnas: Adversarial neural architecture search for gans. In *Proceedings of the IEEE/CVF Conference on Computer Vision and Pattern Recognition*, pp. 5680–5689, 2020.
- Golatkar, A., Achille, A., and Soatto, S. Time matters in regularizing deep networks: Weight decay and data augmentation affect early learning dynamics, matter little near convergence. In *NeurIPS*, 2019.
- Gong, X., Chang, S., Jiang, Y., and Wang, Z. Autogan: Neural architecture search for generative adversarial networks. In *Proceedings of the IEEE International Conference on Computer Vision*, pp. 3224–3234, 2019.
- Goodfellow, I. J., Pouget-Abadie, J., Mirza, M., Xu, B., Warde-Farley, D., Ozair, S., Courville, A., and Bengio, Y. Generative adversarial networks. *arXiv preprint arXiv:1406.2661*, 2014.
- Grinblat, G. L., Uzal, L. C., and Granitto, P. M. Class-splitting generative adversarial networks. *arXiv preprint arXiv:1709.07359*, 2017.
- Gui, J., Sun, Z., Wen, Y., Tao, D., and Ye, J. A review on generative adversarial networks: Algorithms, theory, and applications. *arXiv preprint arXiv:2001.06937*, 2020.
- Gulrajani, I., Ahmed, F., Arjovsky, M., Dumoulin, V., and Courville, A. C. Improved training of wasserstein gans. In *Advances in neural information processing systems*, pp. 5767–5777, 2017.
- Han, K., Wang, Y., Chen, H., Chen, X., Guo, J., Liu, Z., Tang, Y., Xiao, A., Xu, C., Xu, Y., et al. A survey on visual transformer. *arXiv preprint arXiv:2012.12556*, 2020.

- He, H., Wang, H., Lee, G.-H., and Tian, Y. Probgan: Towards probabilistic gan with theoretical guarantees. In *ICLR (Poster)*, 2019.
- Heusel, M., Ramsauer, H., Unterthiner, T., Nessler, B., and Hochreiter, S. Gans trained by a two time-scale update rule converge to a local nash equilibrium. *arXiv preprint arXiv:1706.08500*, 2017.
- Hoang, Q., Nguyen, T. D., Le, T., and Phung, D. Mgan: Training generative adversarial nets with multiple generators. In *International conference on learning representations*, 2018.
- Isola, P., Zhu, J.-Y., Zhou, T., and Efros, A. A. Image-to-image translation with conditional adversarial networks. In *Proceedings of the IEEE conference on computer vision and pattern recognition*, pp. 1125–1134, 2017.
- Jiang, Y., Gong, X., Liu, D., Cheng, Y., Fang, C., Shen, X., Yang, J., Zhou, P., and Wang, Z. Enlightengan: Deep light enhancement without paired supervision. *IEEE Transactions on Image Processing*, 30:2340–2349, 2021.
- Jolicœur-Martineau, A. The relativistic discriminator: a key element missing from standard gan. *arXiv preprint arXiv:1807.00734*, 2018.
- Karras, T., Aila, T., Laine, S., and Lehtinen, J. Progressive growing of gans for improved quality, stability, and variation. *arXiv preprint arXiv:1710.10196*, 2017.
- Karras, T., Laine, S., and Aila, T. A style-based generator architecture for generative adversarial networks. In *Proceedings of the IEEE conference on computer vision and pattern recognition*, pp. 4401–4410, 2019.
- Karras, T., Aittala, M., Hellsten, J., Laine, S., Lehtinen, J., and Aila, T. Training generative adversarial networks with limited data. *arXiv preprint arXiv:2006.06676*, 2020a.
- Karras, T., Laine, S., Aittala, M., Hellsten, J., Lehtinen, J., and Aila, T. Analyzing and improving the image quality of stylegan. In *Proceedings of the IEEE/CVF Conference on Computer Vision and Pattern Recognition*, pp. 8110–8119, 2020b.
- Krizhevsky, A., Hinton, G., et al. Learning multiple layers of features from tiny images. 2009.
- Kupyn, O., Budzan, V., Mykhailych, M., Mishkin, D., and Matas, J. Deblurgan: Blind motion deblurring using conditional adversarial networks. In *Proceedings of the IEEE conference on computer vision and pattern recognition*, pp. 8183–8192, 2018.
- Kurach, K., Lučić, M., Zhai, X., Michalski, M., and Gelly, S. A large-scale study on regularization and normalization in gans. In *International Conference on Machine Learning*, pp. 3581–3590. PMLR, 2019.
- Ledig, C., Theis, L., Huszár, F., Caballero, J., Cunningham, A., Acosta, A., Aitken, A., Tejani, A., Totz, J., Wang, Z., et al. Photo-realistic single image super-resolution using a generative adversarial network. In *Proceedings of the IEEE conference on computer vision and pattern recognition*, pp. 4681–4690, 2017.
- Li, C.-L., Chang, W.-C., Cheng, Y., Yang, Y., and Póczos, B. Mmd gan: Towards deeper understanding of moment matching network. In *Advances in neural information processing systems*, pp. 2203–2213, 2017.
- Lin, C. H., Chang, C.-C., Chen, Y.-S., Juan, D.-C., Wei, W., and Chen, H.-T. Coco-gan: Generation by parts via conditional coordinating. In *Proceedings of the IEEE/CVF International Conference on Computer Vision*, pp. 4512–4521, 2019.
- Liu, Z., Luo, P., Wang, X., and Tang, X. Deep learning face attributes in the wild. In *Proceedings of International Conference on Computer Vision (ICCV)*, 2015.
- Lucic, M., Kurach, K., Michalski, M., Bousquet, O., and Gelly, S. Are gans created equal? a large-scale study. In *Proceedings of the 32nd International Conference on Neural Information Processing Systems*, pp. 698–707, 2018.
- Mao, X., Li, Q., Xie, H., Lau, R. Y., Wang, Z., and Paul Smolley, S. Least squares generative adversarial networks. In *Proceedings of the IEEE international conference on computer vision*, pp. 2794–2802, 2017.
- Mescheder, L., Geiger, A., and Nowozin, S. Which training methods for gans do actually converge? *arXiv preprint arXiv:1801.04406*, 2018.
- Miyato, T., Kataoka, T., Koyama, M., and Yoshida, Y. Spectral normalization for generative adversarial networks. *arXiv preprint arXiv:1802.05957*, 2018.
- Nguyen, T. D., Le, T., Vu, H., and Phung, D. Dual discriminator generative adversarial nets. *arXiv preprint arXiv:1709.03831*, 2017.
- Ouyang, X., Cheng, Y., Jiang, Y., Li, C.-L., and Zhou, P. Pedestrian-synthesis-gan: Generating pedestrian data in real scene and beyond. *arXiv preprint arXiv:1804.02047*, 2018.
- Parmar, N., Vaswani, A., Uszkoreit, J., Kaiser, L., Shazeer, N., Ku, A., and Tran, D. Image transformer. In *International Conference on Machine Learning*, pp. 4055–4064. PMLR, 2018.

- Radford, A., Metz, L., and Chintala, S. Unsupervised representation learning with deep convolutional generative adversarial networks. *arXiv preprint arXiv:1511.06434*, 2015.
- Roth, K., Lucchi, A., Nowozin, S., and Hofmann, T. Stabilizing training of generative adversarial networks through regularization. In *Advances in neural information processing systems*, pp. 2018–2028, 2017.
- Salimans, T., Goodfellow, I., Zaremba, W., Cheung, V., Radford, A., and Chen, X. Improved techniques for training gans. *arXiv preprint arXiv:1606.03498*, 2016.
- Shi, W., Caballero, J., Huszár, F., Totz, J., Aitken, A. P., Bishop, R., Rueckert, D., and Wang, Z. Real-time single image and video super-resolution using an efficient sub-pixel convolutional neural network. In *Proceedings of the IEEE conference on computer vision and pattern recognition*, pp. 1874–1883, 2016.
- Song, K., Tan, X., Qin, T., Lu, J., and Liu, T.-Y. MpNet: Masked and permuted pre-training for language understanding. *arXiv preprint arXiv:2004.09297*, 2020.
- Tian, Y., Wang, Q., Huang, Z., Li, W., Dai, D., Yang, M., Wang, J., and Fink, O. Off-policy reinforcement learning for efficient and effective gan architecture search. In *European Conference on Computer Vision*, pp. 175–192. Springer, 2020.
- Touvron, H., Cord, M., Douze, M., Massa, F., Sablayrolles, A., and Jégou, H. Training data-efficient image transformers & distillation through attention. *arXiv preprint arXiv:2012.12877*, 2020.
- Tran, N.-T., Bui, T.-A., and Cheung, N.-M. Dist-gan: An improved gan using distance constraints. In *Proceedings of the European Conference on Computer Vision (ECCV)*, pp. 370–385, 2018.
- Ulyanov, D., Vedaldi, A., and Lempitsky, V. Deep image prior. In *Proceedings of the IEEE Conference on Computer Vision and Pattern Recognition (CVPR)*, June 2018.
- Vaswani, A., Shazeer, N., Parmar, N., Uszkoreit, J., Jones, L., Gomez, A. N., Kaiser, Ł., and Polosukhin, I. Attention is all you need. In *Advances in neural information processing systems*, pp. 5998–6008, 2017.
- Wang, S., Li, B., Khabsa, M., Fang, H., and Ma, H. Linformer: Self-attention with linear complexity. *arXiv preprint arXiv:2006.04768*, 2020.
- Wang, W., Sun, Y., and Halgamuge, S. Improving mmd-gan training with repulsive loss function. *arXiv preprint arXiv:1812.09916*, 2018a.
- Wang, X., Girshick, R., Gupta, A., and He, K. Non-local neural networks. In *Proceedings of the IEEE conference on computer vision and pattern recognition*, pp. 7794–7803, 2018b.
- Warde-Farley, D. and Bengio, Y. Improving generative adversarial networks with denoising feature matching. 2016.
- Wu, B., Xu, C., Dai, X., Wan, A., Zhang, P., Tomizuka, M., Keutzer, K., and Vajda, P. Visual transformers: Token-based image representation and processing for computer vision. *arXiv preprint arXiv:2006.03677*, 2020.
- Yang, F., Yang, H., Fu, J., Lu, H., and Guo, B. Learning texture transformer network for image super-resolution. In *Proceedings of the IEEE/CVF Conference on Computer Vision and Pattern Recognition*, pp. 5791–5800, 2020.
- Yang, J., Kannan, A., Batra, D., and Parikh, D. Lr-gan: Layered recursive generative adversarial networks for image generation. *arXiv preprint arXiv:1703.01560*, 2017.
- Yang, S., Wang, Z., Wang, Z., Xu, N., Liu, J., and Guo, Z. Controllable artistic text style transfer via shape-matching gan. In *Proceedings of the IEEE International Conference on Computer Vision*, pp. 4442–4451, 2019.
- Yu, J., Lin, Z., Yang, J., Shen, X., Lu, X., and Huang, T. S. Generative image inpainting with contextual attention. In *Proceedings of the IEEE conference on computer vision and pattern recognition*, pp. 5505–5514, 2018.
- Zeng, Y., Fu, J., and Chao, H. Learning joint spatial-temporal transformations for video inpainting. In *ECCV*. Springer, 2020.
- Zhang, H., Goodfellow, I., Metaxas, D., and Odena, A. Self-attention generative adversarial networks. In *International conference on machine learning*, pp. 7354–7363. PMLR, 2019a.
- Zhang, H., Zhang, Z., Odena, A., and Lee, H. Consistency regularization for generative adversarial networks. *arXiv preprint arXiv:1910.12027*, 2019b.
- Zhao, H., Jiang, L., Jia, J., Torr, P., and Koltun, V. Point transformer. *arXiv preprint arXiv:2012.09164*, 2020a.
- Zhao, S., Liu, Z., Lin, J., Zhu, J.-Y., and Han, S. Differentiable augmentation for data-efficient gan training. *arXiv preprint arXiv:2006.10738*, 2020b.
- Zhu, J.-Y., Park, T., Isola, P., and Efros, A. A. Unpaired image-to-image translation using cycle-consistent adversarial networks. In *Proceedings of the IEEE international conference on computer vision*, pp. 2223–2232, 2017a.

Zhu, J.-Y., Zhang, R., Pathak, D., Darrell, T., Efros, A. A., Wang, O., and Shechtman, E. Toward multimodal image-to-image translation. In *Advances in neural information processing systems*, pp. 465–476, 2017b.

Zhu, X., Su, W., Lu, L., Li, B., Wang, X., and Dai, J. Deformable detr: Deformable transformers for end-to-end object detection. *arXiv preprint arXiv:2010.04159*, 2020.

A. Implementation Details

A.1. Specific Setting of Transformer/CNN Combinations

In Sec. 3.1.4, we evaluate the performance of transformer-based G and D by studying four combinations: i) AutoGAN G + AutoGAN D (original AutoGAN); ii) Transformer G + AutoGAN D ; iii) AutoGAN G + Transformer D ; and iv) Transformer G + Transformer D (TransGAN-S). Since the best hyperparameter setting for each combination is different, we list the specific setting in Table. 7. The most noticeable difference is that we apply hinge loss for AutoGAN D following the original paper (Gong et al., 2019), and switch to wgan-gp (Gulrajani et al., 2017) loss when applying Transformer D as the discriminator. This is due to that AutoGAN D contains Spectral Normalization (SN) (Miyato et al., 2018) layer but Transformer D does not. And we apply wgan-gp loss for Transformer D to achieve the similar goal, the Lipschitz constraint. Here we do not make any change of the AutoGAN architectures. We apply Adam optimizer for all four combinations.

Table 7. Detailed setting of four combinations.

Combination	Loss	lr	IS	FID
i)	hinge loss	$2e - 4$	8.55	12.42
ii)	hinge loss	$2e - 4$	8.59	13.23
iii)	wgan-gp	$1e - 4$	6.17	49.83
iv)	wgan-gp	$1e - 4$	6.95	41.41

A.2. Experiments on STL-10 and CelebA 64 x 64

Due to that STL-10 and CelebA datasets contain higher resolution images (e.g., 48×48 and 64×64), the memory cost of TransGAN will also increase. As discussed in Sec. 3.5, since increasing the model size of TransGAN’s generator shows a more significant improvement than the multi-task co-training (MT-CT) strategy, we remove the MT-CT loss in order to save the memory for a larger model.

B. Network Architecture

We include the specific architecture configurations of TransGAN-XL in Table. 8 9. The “Encoder” represents

the basic Transformer Encoder block constructed by self-attention, LayerNormalization, and Feed-forward MLP. PixelShuffle layer is adopted for feature map upsampling. “input_shape” and “output_shape” denotes the shape of input feature map and output feature map, respectively.

Table 8. Specific configuration of the generator of TransGAN-XL

Stage	Layer Type	input_shape	output_shape
-	MLP	1024	$(8 \times 8) \times 1024$
1	Encoder	$(8 \times 8) \times 1024$	$(8 \times 8) \times 1024$
	Encoder	$(8 \times 8) \times 1024$	$(8 \times 8) \times 1024$
	Encoder	$(8 \times 8) \times 1024$	$(8 \times 8) \times 1024$
	Encoder	$(8 \times 8) \times 1024$	$(8 \times 8) \times 1024$
2	PixelShuffle	$(8 \times 8) \times 1024$	$(16 \times 16) \times 256$
	Encoder	$(16 \times 16) \times 256$	$(16 \times 16) \times 256$
	Encoder	$(16 \times 16) \times 256$	$(16 \times 16) \times 256$
	Encoder	$(16 \times 16) \times 256$	$(16 \times 16) \times 256$
3	PixelShuffle	$(16 \times 16) \times 256$	$(32 \times 32) \times 64$
	Encoder	$(32 \times 32) \times 64$	$(32 \times 32) \times 64$
	Encoder	$(32 \times 32) \times 64$	$(32 \times 32) \times 64$
-	Linear Layer	$(32 \times 32) \times 64$	$32 \times 32 \times 3$

Table 9. The specific configuration of the discriminator of TransGAN-XL

Stage	Layer Type	input_shape	output_shape
-	Linear Flatten	$32 \times 32 \times 3$	$(8 \times 8 + 1) \times 384$
1	Encoder	$(8 \times 8 + 1) \times 384$	$(8 \times 8 + 1) \times 384$
	Encoder	$(8 \times 8 + 1) \times 384$	$(8 \times 8 + 1) \times 384$
	Encoder	$(8 \times 8 + 1) \times 384$	$(8 \times 8 + 1) \times 384$
	Encoder	$(8 \times 8 + 1) \times 384$	$(8 \times 8 + 1) \times 384$
	Encoder	$(8 \times 8 + 1) \times 384$	$(8 \times 8 + 1) \times 384$
	Encoder	$(8 \times 8 + 1) \times 384$	$(8 \times 8 + 1) \times 384$
-	-	$(8 \times 8 + 1) \times 384$	1×384
-	Classification Head	1×384	1

C. Benchmark CelebA 64 x 64

As discussed in Sec. 3, due to that scaling up the model size of generator introduce a more significant improvement than the multi-task co-training (MT-CT) strategy, we remove the MT-CT loss on CelebA experiments to save the memory for a large-size generator. We then compare the performance of TransGAN with current ConvNet-based GAN on CelebA 64 x 64 dataset, shown in Table. 10

D. Data Augmentation Strategy

We mainly follow the way of differentiable augmentation (Zhao et al., 2020b) to apply the data augmentation on our GAN training framework. Specifically, we conduct $\{Transition, Cutout, Color\}$ augmentation for Trans-

Table 10. Comparison on CelebA 64 x 64.

METHODS	FID
DCGAN (RADFORD ET AL., 2015) + TTUR (HEUSEL ET AL., 2017)	12.50
COCO-GAN (LIN ET AL., 2019)	4.00
TRANSGAN-XL	12.23

GAN with probability p , while p is empirically set to be $\{1.0, 0.3, 1.0\}$. However, we find that *Transition* augmentation will hurt the performance of ConvNet-based GAN when 100% data is utilized. Therefore, we remove it and only conduct $\{Cutout, Color\}$ augmentation for AutoGAN (Gong et al., 2019).

E. Efficiency Comparing with ConvNet

We further compare the computational cost of TransGAN with current state-of-the-art ConvNets, including both the small model TransGAN-S and largest model TransGAN-XL. As shown in Table. 11, we firstly compare TransGAN-S with SN-GAN (Miyato et al., 2018), since they achieve similar performance. Specifically, TransGAN-s reaches a similar IS score and better FID score comparing with SN-GAN, while only costs about half FLOPs of SN-GAN. We then compare our largest model TransGAN-XL⁺ with AutoGAN (Gong et al., 2019) and Progressive-GAN (Karras et al., 2017). TransGAN-XL⁺ reaches best FID score with much smaller FLOPs compared to Progressive GAN and slightly large FLOPs (1.06G) compared to AutoGAN.

 Table 11. Efficiency comparison between TransGAN and ConvNet-based methods. Results are reported on Cifar-10 dataset with 32×32 resolution.

METHODS	FLOPS (G)	IS	FID
SNGAN (MIYATO ET AL., 2018)	1.57	8.22 ± 0.05	21.7
TRANSGAN-S	0.68	8.22 ± 0.14	18.58
AUTOGAN (GONG ET AL., 2019)	1.77	8.55 ± 0.10	12.42
PROGRESSIVE-GAN (KARRAS ET AL., 2017)	6.39	8.80 ± 0.05	15.52
TRANSGAN-XL	2.83	8.63 ± 0.12	11.89